2-17-2015

Directed Evolution of a Yeast-Displayed HIV-1 SOSIP gp140 Spike Protein toward Improved Expression and Affinity for Conformational Antibodies

Sebastian K. Grimm
Dartmouth College

Michael B. Battles
Dartmouth College

Margaret E. Ackerman
Dartmouth College

Directed Evolution of a Yeast-Displayed HIV-1 SOSIP gp140 Spike Protein toward Improved Expression and Affinity for Conformational Antibodies

Sebastian K. Grimm, Michael B. Battles, Margaret E. Ackerman*

Thayer School of Engineering at Dartmouth, Hanover, New Hampshire, United States of America

* margaret.e.ackerman@dartmouth.edu

Abstract

Design of an envelope-based immunogen capable of inducing a broadly neutralizing antibody response is thought to be key to the development of a protective HIV-1 vaccine. However, the broad diversity of viral variants and a limited ability to produce native envelope have hampered such design efforts. Here we describe adaptation of the yeast display system and use of a combinatorial protein engineering approach to permit directed evolution of HIV envelope variants. Because the intrinsic instability and complexity of this trimeric glycoprotein has greatly impeded the development of immunogens that properly represent the structure of native envelope, this platform addresses an essential need for methodologies with the capacity to rapidly engineer HIV spike proteins towards improved homogeneity, stability, and presentation of neutralizing epitopes. We report for the first time the display of a designed SOSIP gp140 on yeast, and the *in vitro* evolution of derivatives with greatly improved expression and binding to conformation-dependent antibodies. These efforts represent an initial and critical step toward the ability to rapidly engineer HIV-1 envelope immunogens via directed evolution.

Introduction

Broadly neutralizing antibodies (bnAbs) are widely thought to represent the best means of preventing HIV infection, making development of an immunogen capable of raising bnAbs a cornerstone and priority of vaccine development efforts [1,2]. Unfortunately, various factors relating both to the characteristics of known bnAbs as well as the HIV virus itself have pointed toward substantial obstacles to the realization of this goal. The sequence diversity and instability of the trimer, its heavily glycosylated structure, low surface density on the viral particle, and limited access to functionally critical epitopes have confounded efforts to induce bnAbs by vaccination [1,3]. Furthermore, cues from natural infection suggest that monoclonal bnAbs are uncommon, arise after years of infection and high viral load, fail to control established infection, must have precisely oriented binding interactions, and often have unusual properties

[4–11], indicating that without a fundamental breakthrough in immunogen design, the generation of such bnAbs by vaccination is likely to remain a daunting challenge [12,13].

Even so, exciting progress has been achieved recently in characterizing the neutralizing capacity of antibodies generated in the course of natural infection [11,14–17], as well as in identifying novel bnAbs [18–27]. These and other bnAbs have greatly informed immunogen design, highlighting new regions of the envelope trimer, variable loops, envelope glycan, the membrane proximal region, novel quaternary epitopes, and receptor and co-receptor binding sites as epitopes with a combination of sufficient conservation and functional relevance to be key targets of an effective antibody response. It is anticipated that with the continued use of high-throughput B-cell screening methods, the set of bnAbs with different fine-epitope specificities and viral coverage will continue to grow and provide a rich set of probes to reinvigorate and diversify immunogen design efforts. However, a high-throughput and adaptable platform is required to ensure these findings are efficiently translated into candidate immunogen development.

In the context of natural infection, bnAbs have tended to be isolated from individuals with high viral loads, persistent antigen exposure, and progressive disease. In the absence of replicating vectors, it is difficult to envision how similar levels of antigen exposure could be accomplished via vaccination. Additionally, envelope diversity may be a key driver in the generation of neutralization breadth, posing another fundamental challenge. Together, the antigen exposure associated with natural infection likely represents both orders of magnitude greater levels and diversity than can be achieved by current strategies, leading to the discouraging conclusion that a successful immunogen may need to possess an orders of magnitude improved capacity to elicit bnAbs over natural envelope.

With these technical and immunological gaps in mind, we sought to establish a yeast surface display (YSD) platform to apply directed molecular evolution principles to the development of HIV envelope variants with fundamentally improved biophysical properties. YSD allows the display of millions of sequence variants and selection based on flexible design criteria to allow efficient and deep coverage of the envelope structure:function landscape, representing a potentially enabling technology for the rapid translation of findings from basic studies to the development of novel candidate immunogens. As such, YSD has been established as a powerful method to engineer diverse proteins for a broad range of functional improvements, including stability, specificity, affinity, catalysis, and enantioselectivity [28–31]. Routinely, variants with million-fold improvements can be isolated from large libraries, and repeated cycling of mutagenesis and selection has resulted in evolution of some of the highest affinity synthetic interactions ever observed [32]. Indeed, promising efforts aimed at the development of scaffolded epitopes and gp120 cores with desirable properties such as enhanced recognition of germline antibody families have routinely relied upon such combinatorial approaches and YSD-based directed evolution [33,34]. However, yeast expression and display of complete gp120, much less gp140, has not been described.

Here we investigated yeast as a host for the display of HIV spike protein variants and report for the first time the display of full-length gp140 on *S. cerevisiae*. A JR-FL gp140 variant with the SOSIP mutations served as starting point because it has previously been engineered for stability and homogeneity, was well-expressed in mammalian cells [35–37] and because the SOSIP mutations proved key to enabling structural insights into the native HIV-1 envelope trimer [38–41]. We have applied random mutagenesis and DNA shuffling in combination with stringent VRC01 driven selections to isolate gp140 SOSIP variants with significantly enhanced expression and that bind to conformational HIV bnAbs, suggesting proper antigenicity. The yeast-displayed gp140 SOSIP variants described here demonstrate the feasibility of production of HIV envelope in yeast, and the advantages of this robust platform in evolving variant

envelopes. If trimeric presentation can be confirmed or further engineered, YSD may prove a robust platform for the rapid evolution and selection of promising vaccine immunogens.

Results

Influence of N-glycosylation on binding of conformational HIV antibodies to yeast-produced gp120

Since HIV spike proteins are highly glycosylated, proteolytically processed, and contain numerous disulfide bonds, only eukaryotic cells with appropriate protein processing machinery can serve as hosts for the display of functional protein. Whereas mammalian cell lines are relatively slow growing, and achieving the single genotype-phenotype linkage requires viral transfections or other rather cumbersome and time-consuming methodologies, the yeast *S. cerevisiae* is a robust and well-described eukaryotic host for cell-surface display [42]. Yeast are capable of displaying complex mammalian glycoproteins such as antibody fragments, full-length antibodies, peptide-MHC molecules, or growth factor receptors [42–45], as well as a growing number of viral envelope proteins of fragments thereof such as hemagglutinin, the gp120 core, Dengue E protein, SARS-CoV, West Nile Virus envelope, and the Hepatitis C Virus envelope protein E2 [46–51], suggesting that the display of HIV envelope protein is feasible in principle. Nevertheless, in *S. cerevisiae*, N-linked glycans are extended and mannose-rich [52], though *P. pastoris* yeast strains with human or human-like N-linked glycosyation have been reported to overcome this limitation [53,54].

To investigate whether heterologous N-glycosylation in yeast has a major effect on the recognition of gp120 by conformational antibodies, we compared HIV-1 JR-FL gp120 produced in either *S. cerevisiae* strain YVH10 or glycan-engineered *P. pastoris* [53] for binding to a panel of conformational HIV-1 bnAbs. The mannose-rich N-glycosylation in YVH10 is trimmed to a more human-like 5-mannose stem in engineered *Pichia*, which may promote proper protein folding and conformational Ab recognition. However, we found that *Pichia*-produced gp120 did not display a clearly improved binding profile across a panel of bnAbs (S1 Fig.). Furthermore, *P. pastoris*-produced gp120 appeared somewhat more fragmented on a Western blot, suggesting more proteolytic degradation as compared to *S. cerevisiae*. Therefore, and because of the well-established and characterized Aga1/2-based display system, *S. cerevisiae* was chosen as host for HIV spike protein display.

Design of a codon-optimized gp140 for expression in *S. cerevisiae*

Since the secretion of a full-length JR-FL gp140 including the stabilizing SOS and I559P substitutions (SOSIP JR-FL gp140 [36,37]) in *S. cerevisiae* YVH10 had failed, we fragmented the gene and compared the level of secreted protein between a gp120 stripped core construct described previously [47], gp120 trimmed at N- and C-termini, full-length gp120, a full-length SOSIP gp140, as well as gp41, and gp41 lacking its hydrophobic fusion peptide (Fig. 1A). Notably, proteins were not secreted as Aga2 fusions in this study. Firstly, both gp120 fragments and full-length gp120 could be secreted at clearly detectable levels, but not full-length SOSIP gp140. Secondly, the omission of the fusion peptide clearly enhanced secretion of gp41, suggesting that its omission or modification may also improve full-length gp140 secretion. Thirdly, gp120 collapsed near its expected MW of 52 kDa after treatment with N-glycosidase PNGase F, suggesting extensive N-glycosylation (Fig. 1B and 1C). Based on these findings, we rationally designed a JR-FL SOSIP-based gp140 (designed, or d-SOSIP) with some modifications: codons were optimized for *S. cerevisiae* [55]; hydrophobic amino acids within the fusion peptide were replaced by structurally related but more hydrophilic residues, which if possible were found among circulating viral sequences (Fig. 1D); and lastly the Furin protease cleavage site was substituted with a yeast Kex2
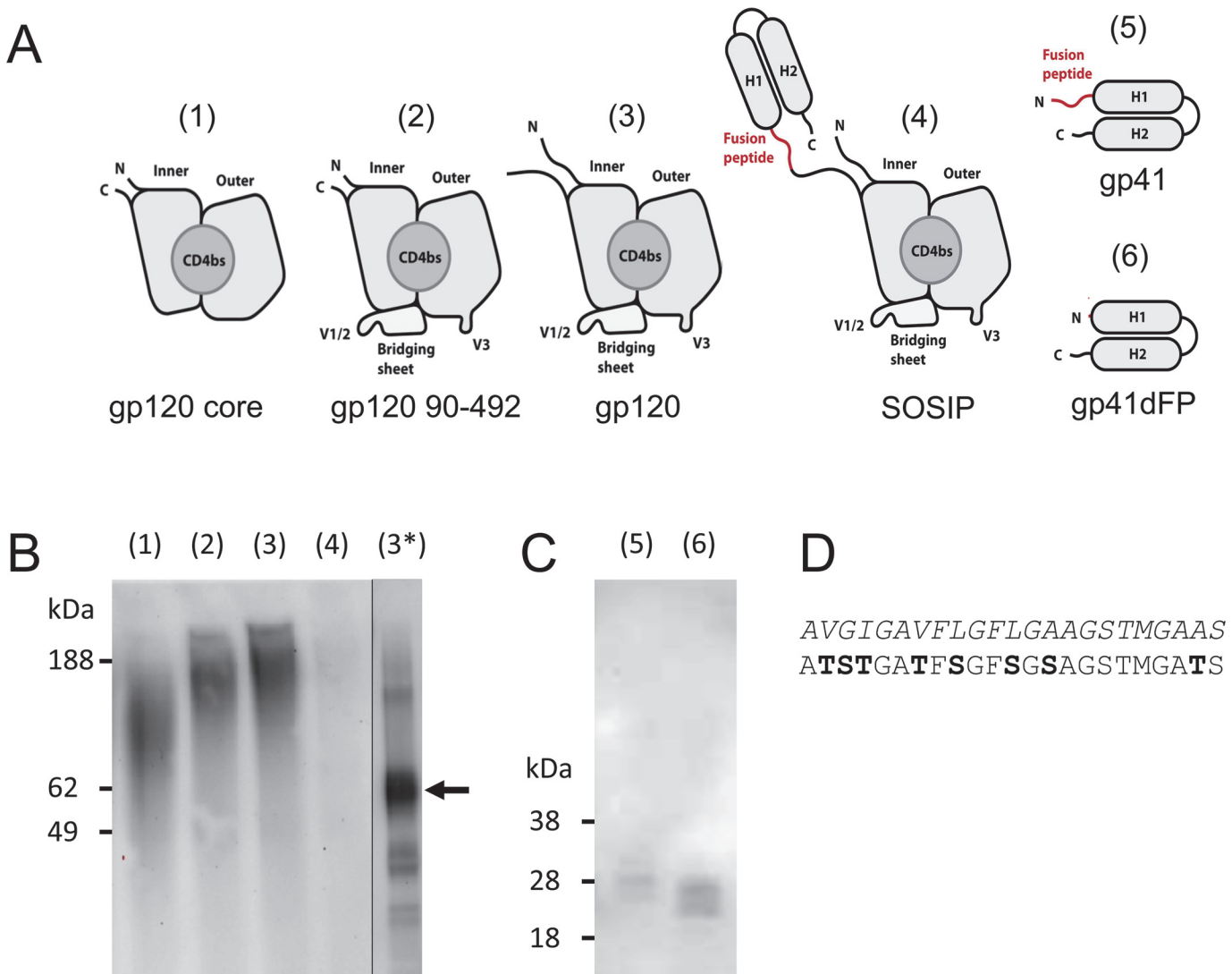
Fig 1. Expression analysis of different gp140 fragments. (A) Schematic representations of expressed HIV-1 gp140 fragments, including gp120 inner and outer domain (inner and outer), CD4 binding site (CD4bs), V1/2 loop region (V1/2), the V3 loop (V3) and helical regions 1 and 2 of gp41 (H1, H2). (B) Western blot analysis of (1) yeast-secreted YU2 gp120 core, (2) gp120 residues 90–492, (3) gp120, (4) JR-FL SOSIP gp140, (3*) PNGaseF-treated YU2 gp120 with marked main band. Lane (3*) is non-adjacent but originates from the same blot. (C) Western blot analysis of (5) yeast-secreted JR-FL gp41 and (6) gp41 lacking the fusion peptide. (D) Amino acid sequences of the original and the modified fusion peptide, with modified residues in bold text.

doi:10.1371/journal.pone.0117227.g001

recognition site, and a predicted internal Kex2 site was removed. We then compared secreted protein content in cell culture supernatant and found that d-SOSIP, but not the initial JR-FL SOSIP gp140 could be detected at significant levels. The d-SOSIP variant was significantly N-glycosylated, and collapsed after PNGase F-treatment (S1C Fig.).

Characterization of d-SOSIP displayed on *S. cerevisiae*

The rationally designed d-SOSIP variant and a mutant with disrupted CD4 binding site (CD4bs)-specific Ab binding (d-SOSIP D368R) were displayed as Aga2 fusion proteins on yeast (Fig. 2A), and compared for display level and binding to a panel of HIV bnAbs together with the well-characterized and folded YU2 gp120 core [47] and an unrelated viral envelope protein (E2) derived from Hepatitis C virus (HCV E2) as positive and negative controls

Fig 2. Binding analysis of yeast-displayed spike protein variants. (A) Schematic illustration of yeast-displayed gp140 that is C-terminally fused to Aga2. (B) Overlay of histograms obtained from *S. cerevisiae* displaying JR-FL d-SOSIP gp140 (d-SOSIP), JR-FL d-SOSIP gp140 D368R mutant (d-SOSIP D368R), YU2 gp120 core (gp120 core) or an Hepatitis C Virus reference protein (HCV E2) probed for display level. Counts are plotted against fluorescence on logarithmic scale. (C) Overlay of histograms of yeast-displayed constructs binding to 100 nM HIV bnAb VRC01. (D) Median fluorescence intensities (MFI) normalized for yeast display levels (nMFI) are plotted for a panel of HIV Abs, grouped by epitope (CD4bs = CD4 binding site; V loop = variable loops V1/2/3; MPER = membrane proximal extracellular region; and G = glycan-specific). Error bars represent standard deviations of triplicate measurements.

doi:10.1371/journal.pone.0117227.g002

(Fig. 2). Notably, gp120 core epitopes are included in d-SOSIP, while the gp120 core lacks many of the epitopes of d-SOSIP, including variable loop and gp41-associated epitopes (Fig. 1A). Induced yeast cells always included a population that did not display the heterologous protein, which is a feature of the Aga2 display system [42]. The d-SOSIP constructs showed extremely low display levels as compared to the gp120 core (Fig. 2B), and only somewhat above background binding of the CD4bs-specific VRC01 Ab (Fig. 2C). However, standardizing the binding of HIV-specific Abs when variable display level was taken into account

lead to detectable binding across a wide range of Ab specificities, including conformational, linear, and glycan-dependent sites. Yeast-displayed d-SOSIP bound well to the V3-specific Ab 447–52D and to MPER Abs, as might be expected due to their ability to bind to unconstrained peptides. Surprisingly, low but reproducible signal was observed, suggestive of recognition by glycan and trimer-preferring antibodies such as PGT121/126 [56] and PG9/16 [24] (Fig. 2D and S2 Table). Furthermore, the d-SOSIP D368R substitution was observed to reduce binding of CD4bs antibodies. Nonetheless, the low signal relative to gp120 core for many of the antibodies tested clearly indicated significant room for improvement, which might be achieved by coupling the rational design modifications made thus far with directed evolution strategies.

Selection of gp140 variants with improved binding to conformational mAbs

To select for properly folded sequence variants of d-SOSIP, a library of 2.0×10^7 members was prepared, with each library member containing an average of about 6.7 random amino acid mutations (Table 1). Conformation-dependent mAbs that specifically bind to discontinuous epitopes served as molecular probes for properly folded antigens. Here, the d-SOSIP library was extensively screened for improved binding to the conformation-dependent CD4bs bnAb VRC01, which mimics the natural ligand CD4 in its mode of binding[57]. The pool of clones selected was further diversified to up to 7.7×10^7 members during two additional cycles of error prone PCR and repeated FACS selection for improved binding to either VRC01 (track 1), alternating enrichment based on binding to HIV CD4bs Abs VRC01, CH31 or PGV04 (track 2), or against a pooled mix of the five CD4bs mAbs VRC01, PGV04, CH31, b12 and b6 (track 3), as described in Table 1. These mAbs were chosen because they all bind to the conformational, conserved and functionally critical CD4bs, while being different in sequence and paratope, so as to minimize the risk of selecting specific affinity-enhancing contact residues instead of general structurally stabilizing mutations. A comparative binding analysis of the initial d-SOSIP and the selected pools from cycle 2 onward showed enhanced binding not only to target bnAb VRC01, but also to non-target CD4bs mAb b6, suggesting a generally improved structural representation of the conformational CD4bs epitope (Fig. 3B), as VRC01 and b6 significantly differ in their epitope footprints within the CD4bs [58,59]. DNA sequencing revealed that two dominating and distinct clusters of sequences had been enriched (S3A Fig.). To select for

**Table 1. Summary of library size, diversity, and selection parameters and paths.**

Cycle	Method	Size	Mutations	Track (1)	Track (2)	Track (3)	Counter selection
1.1	epPCR, FACS	2.0×10^7	6.7 aa/gene	256 nM VRC01	-	-	No
1.2	FACS	-	-	256 nM VRC01	-	-	No
1.3	FACS	-	-	128 nM VRC01	-	-	No
2.1	epPCR, FACS	5.3×10^7	12.3 aa/gene	256 nM VRC01	-	-	No
2.2	FACS	-	-	128 nM VRC01	-	-	No
2.3	FACS	-	-	128 nM VRC01	-	-	No
2.4	FACS	-	-	128 nM VRC01	-	-	Yes
3.1	epPCR, FACS	7.7×10^7	19.0 aa/gene	128 nM VRC01	-	-	No
3.2	FACS	-	-	64 nM VRC01	64 nM PGV04	64 nM Ab mix	No
3.3	FACS	-	-	32 nM VRC01	64 nM CH31	32 nM Ab mix	No
4.1	Shuffling, FACS	6.2×10^7	6.1 aa/gene	32 nM VRC01	32 nM VRC01	32 nM VRC01	No
4.2	FACS	-	-	16 nM VRC01	32 nM CH31	16 nM Ab mix	No
4.3	FACS	-	-	2 nM VRC01	8 nM PGV04	4 nM Ab mix	No

doi:10.1371/journal.pone.0117227.t001
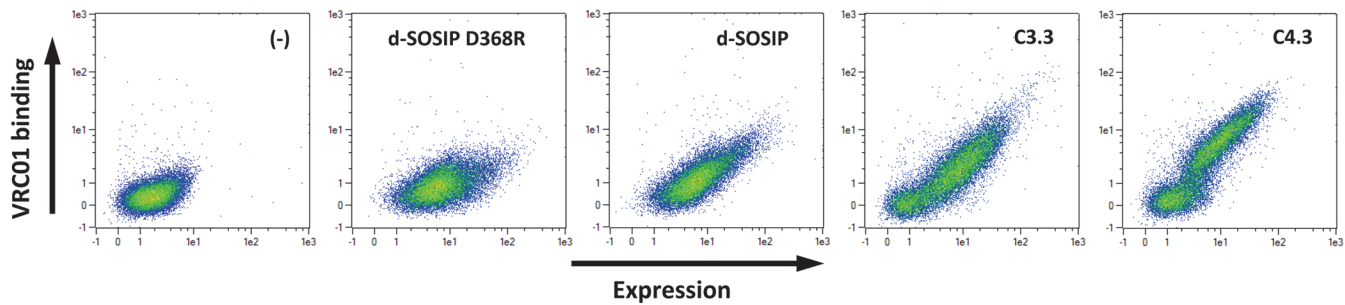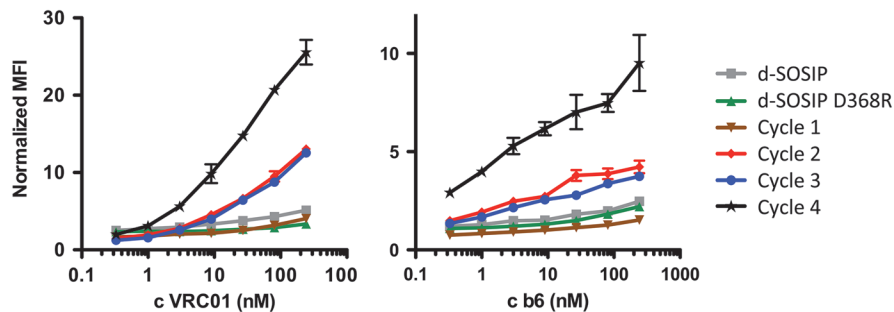
Fig 3. Pool binding analysis of selection rounds. (A) Scatter plots obtained from 20,000 yeast cells displaying no HIV envelope protein (-), d-SOSIP gp140 D368R (d-SOSIP D368R), d-SOSIP or selected pools after cycles C3.3 and C4.3, respectively, probed for binding to 27 nM VRC01. (B) Binding isotherms obtained from pools selected after round 1.3, 2.4, 3.3 and 4.3 (cycle 1, 2, 3, 4), and reference clones d-SOSIP gp140 (d-SOSIP) and d-SOSIP D368R to HIV mAbs VRC01 or b6. Expression-normalized median fluorescence intensity (nMFI) is plotted against antibody concentration. Error bars represent standard deviations of triplicate measurements.

doi:10.1371/journal.pone.0117227.g003

combinatorial mutants with further improved binding properties among those clusters, and to remove structurally disruptive mutations that likely had been co-selected, d-SOSIP and the 3.3 pool variants were DNA-shuffled [60] at a 1:1 ratio, and then subjected to an additional three rounds of FACS following selection tracks 1, 2 and 3. The selected 4.3 population pools showed both greatly enhanced expression and binding to CD4bs mAbs VRC01 and b6 as compared to the 3.3 pool selected before DNA shuffling (Fig. 3), while there was no difference in binding observed between tracks 1, 2 and 3 (S4 Fig.).

Characterization of selected clones

A total 16 clones from each selection track were evaluated for binding to VRC01 and absence of binding to two negative control mAbs. Using an aggregated ranking analysis, the 12 clones with the best VRC01 and least control mAb binding were further screened for broad recognition of conformational CD4bs mAbs PGV04 and b6, as well as the natural ligand CD4 and gp41 membrane-proximal extracellular region mAb 2F5. Two unique clones, denoted 4.3.B01 and 4.3.D01, were identified as ranking best both for binding specificity and breath of HIV-specific mAb/CD4 recognition. DNA sequencing of 4.3.B01, 4.3.D01 and a reference clone that was enriched before DNA shuffling (3.3.1) revealed a total of 17, 12 and 9 amino acid substitutions in 3.3.1, 4.3.B01, and 4.3.D01, respectively. Notably, 4.3.B01 and 4.3.D01 are identical in the gp120 region and only differ by 3 mutations within the gp41 region that were reverted to d-SOSIP wild type for clone 4.3.D01 (S5 Fig.). Both 4.3.B01 and 4.3.D01 showed greatly improved binding to several CD4bs Abs, both neutralizing and non-neutralizing, and also V3 Ab

F425 B4e8 and MPER Ab 2F5, as compared to the initial d-SOSIP. Perhaps surprisingly, improved binding to natural ligand CD4-Fc was not detected, but binding was maintained at a comparable level with d-SOSIP (Fig. 4).

To determine whether the enhancements observed in displayed variants were generalizable to secreted protein, the clone 4.3.D01 was expressed solubly. The evolved variant was subsequently compared to yeast-secreted gp120 for binding to envelope-specific antibodies. Notably, reference d-SOSIP could not be secreted at sufficient quantities in yeast for binding analyses, in line with the extremely low display level of d-SOSIP observed on yeast cells (Figs. 2 and 3). Beyond enabling expression, the 4.3.D01 clone exhibited improved binding to a number of mAbs, notably NIH45–46 G54W, relative to gp120. (S7 Fig.), suggesting that the improved binding properties observed on yeast cells correlate with improved binding properties of soluble gp140.

Mapping selected mutations onto the structure of BG505 SOSIP.664

Mapping of the mutations on the crystal structure of BG505 SOSIP.664 gp140[39] showed that the mutations found in 4.3.B01 and 4.3.D01 cluster in a relatively narrow region within the V1/V2 loop region of gp120, but proximal to the CD4bs (Fig. 5A). Their side chains are buried within the protein or located in small cavities and do not appear to directly contact CD4bs mAbs (Fig. 5B), suggesting that structurally stabilizing mutations have been selected. Interestingly, mutated residues H66Q and W112R may form hydrogen bonds stabilizing helices within the inner domain of gp120. Similarly, I424N may form a novel hydrogen bond with Y384 (Fig. 5C). Mutation N156I disrupts an N-glycosylation motif located within the V1/V2 loop region. Three additional gp120 mutations that were lost after shuffling (T50A, L122F, and S209T) were all surface located, suggesting that surface-located mutations may not be essential to improved protein folding in yeast.
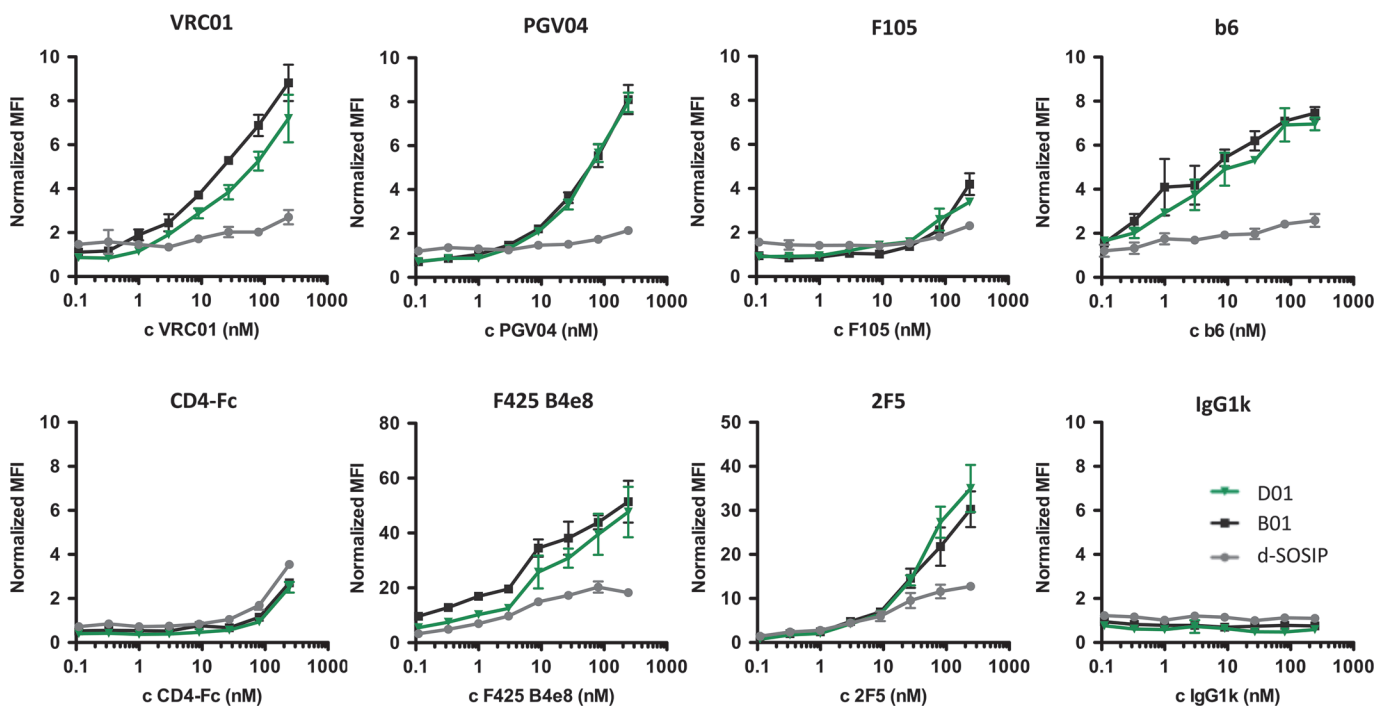
Fig 4. Single clone binding analysis. Expression-normalized median fluorescence intensity (MFI) is plotted against logarithmic Ab concentrations for d-SOSIP (gray) and clones 4.3.B01 (black) and 4.3.D01 (green) selected after DNA shuffling. Binding isotherms to a human IgG1k control Ab are included as reference. Error bars represent standard deviations of triplicate measurements.

doi:10.1371/journal.pone.0117227.g004
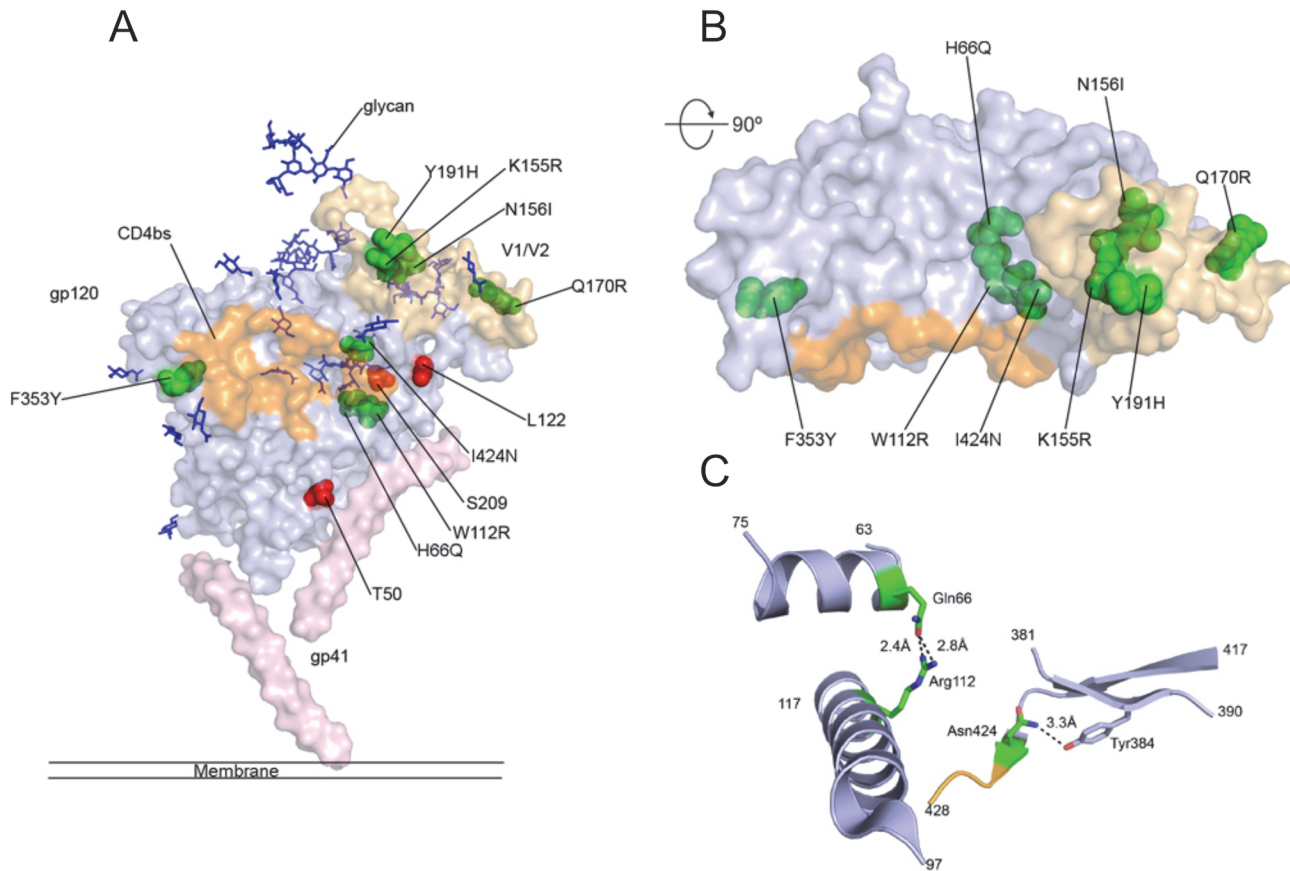
Fig 5. Mapping of mutations on gp140 structure. (A) Surface view of the structure of a BG505 SOSIP.664 gp140 monomer. The gp120 unit is shown in light blue and the gp41 unit in light pink. Glycans are shown as blue sticks, the CD4bs is orange and the V1/2 loop domain golden. Mutated residues found in clone 3.3.1 only are shown in red and residues found in clones 4.3.B01 and 4.3.D01 are shown in green. (B) The molecule was rotated 90° around the x-axis and residues found in 4.3.B01 and 4.3.D01 are shown in green. (C) Cartoon view of mutated residues found within gp120, putative hydrogen bonds are denoted as dashed lines.

The mutations found within gp41 could not be mapped due to disordered electron density in this particular region of the SOSIP crystal structure. Since 4.3.B01 and 4.3.D01 showed virtually identical binding profiles and expression levels (Fig. 4), these gp41 mutations do not appear to strongly contribute to either improved protein expression or Ab recognition.

Discussion

A key attribute of most effective anti-viral vaccine responses is development of antibodies to viral envelope proteins which result in the ability to prevent or clear viral infection [61]. To this end, induction of neutralizing antibodies capable of blocking viral infection has been a cornerstone of HIV vaccine efforts. However, HIV has an arsenal of ways to evade antibody recognition, including multiple conformational states such as closed and open, cleaved or uncleaved trimer and various monomeric spike protein forms, which are thought to distract and dilute the adaptive immune response to the infectious "native" envelope trimer [11,62–64].

Immunogen design efforts aimed to circumvent these barriers stem back to the discovery of the HIV bnAb b12, and began with the identification of epitope mimetic peptides that were capable of binding to b12 with high affinity. However, vaccination with mimetic peptides failed to induce Abs that bound to gp120 [65]. Other more recent approaches have been based on a

subtractive principle, in which the immunogenic features of the antigen which lead to non-neutralizing but immunodominant antibody responses were removed or masked with glycans [58,66,67], or even more dramatically, on the direct grafting of functionally relevant sites onto alternative scaffolds [68–70], with the goal of focusing the immune response on functionally relevant epitopes. The subtraction of alternative epitopes, however, may not actively promote a response against the desired epitope, and may rather result in a blunted immune response, in which the titer of Ab recognizing the selected epitope is not enhanced, but the total antibody response is decreased. While mixed success has recently been reported from these efforts in the setting of HIV [71], the subtraction of epitopes may unnecessarily constrain the immune response—strongly limiting potentially protective recalled T cell responses, and non-productively decreasing the polyclonality of the antibody response, resulting in reduced recruitment of effector mechanisms reliant on avid interactions with antibody opsonized cells or virus. Because these effector mechanisms have a demonstrated importance in preventing acquisition, decreasing viral burden, and delaying progression [72], the possible immunologic outcome of vaccines with reduced epitopic coverage may be dividing rather than conquering.

Extensive studies utilizing soluble gp120 have generally failed to provide protective Ab responses, and numerous full-length and trimeric gp140-based antigens that may better resemble the structure of the native spike have also been tested [73–75], following the rationale that any antibody recognizing the native, trimeric spike should neutralize virus [41]. SOSIP trimers fall into this class, and a growing number of envelope sequences with SOS and IP mutations have been individually constructed and tested, culminating with the BG505 SOSIP.664 gp140 trimer [39].

A complementary approach to the strictly rational development of stable, uniform and well-behaved proteins is combinatorial protein engineering, involving screening of large libraries of protein mutants displayed on viruses or cells for improved properties such as affinity, stability or protein expression. Toward this end, HIV virus particles have been exposed to temperature or chemical denaturant stress and screened for retained infectivity of mammalian cells. More homogeneous and stable viruses could be selected following this procedure [76]. However, cellular protein display methods, yeast display in particular, have standing as the gold-standard for evolution of complex and glycosylated proteins based on advantages in speed, library construction, scalable selections, and ease of use.

Our application of this system to a designed variant of JR-FL SOSIP gp140 represents the first use of a high-throughput platform for whole envelope evolution. The ease with which variants with improved expression and binding to conformational HIV antibodies could be evolved from repeated rounds of random mutagenesis and flow-cytometric selection points toward promising utility. While the mannose-rich glycosylation of *S. cerevesiae* in theory reduces enthusiasm about this host, major classes of bnAbs, including glycan-specific Abs, bound to yeast-produced gp140 variants, and loss of only one N-glycosylation motif (N156I) was observed after selection. While improved binding to CD4 was not observed, the selected variants exhibited similar CD4 binding as gp120 core, and showed broadly improved binding across multiple CD4bs mAbs, suggesting a generally improved structural representation of this epitope.

Whether the selected d-SOSIP variants could elicit improved neutralizing immunity when applied as immunogens is unclear. Because improved antigenicity does not equate to improved immunogenicity, immunization studies would be required to evaluate their ability to elicit neutralizing antibodies. Differences in glycosylation can also have a large impact on antigenicity [17], a factor that has not been optimized in our study. Importantly, while yeast utilize the same glycosylation motif, the composition of the glycan incorporated differs significantly, and could be engineered. We rather consider the methodology described here and gp140 variants

as an enabling platform for future investigations towards development of improved immunogens. A panel of diverse, stabilized gp140 variants is thought to likely be required to cover circulating virus diversity, minimize immune escape by mutation and glycan masking, and elicit broad neutralization activity [15].

The nine mutations within gp120 that contributed to the enhanced properties in yeast are located in a relatively narrow region, either in proximity of the CD4bs or within the V1/V2 loop domain, as determined by homology modeling. Interestingly, three of the nine mutations (H66Q, W112R and I424N) may form novel hydrogen bonds. The predominantly buried locations of the mutations identified and the predicted presence of additional, buried hydrogen bonds in selected clones suggest that the poor surface display level and limited binding of yeast-displayed gp140 to conformational Abs observed initially were related to poor folding of gp140 in *S. cerevisiae*, and that improved gp120 core packing and hydrogen bonding within the core may have helped to stabilize the protein, enhancing folding and resulting in higher display levels. In fact, the display level of proteins fused to Aga2p was shown previously to correlate with their thermal stability and soluble expression levels [77], and yeast is known to contain a chaperone machinery that can retain and degrade misfolded protein [78]. Further, the accumulation of mutations within the V1/V2 loop domain suggest that this region, in addition to the gp120 core itself, had a critical impact on obstructing proper folding of gp120. This finding is further supported by the notion that yeast produced gp120 core lacking this domain binds well to CD4bs conformational Abs, while full-length gp120 containing V1/V2 did not. The more hydrophilic gp41 fusion peptide has provided a critical handle to rationally improve expression of d-SOSIP gp140 in *S. cerevisiae*, however no additional expression enhancing or apparently structurally stabilizing gp41 mutations were identified in the evolved d-SOSIP gp140 variants. Evidence as to the utility of these rational mutations can be found in the absence of reversions observed among selected clones.

Notably, this study does not provide any evidence for the display of gp140 trimers on yeast, which from a steric perspective seems unlikely due to clashes of the Aga2 cell wall anchoring fusion partners. Further, the engineering of the fusion peptide towards reduced hydrophobicity may, while being as conservative as possible, have an effect on an overall trimer structure. To address this, in future studies, a secretion-capture-based display system could be developed [79], allowing for the evolution of trimeric gp140 spike protein libraries that are non-covalently linked to Aga2. The engineered fusion peptide could gradually be mutated back to wild-type if it affects trimer structure, or fusion peptide variants could be selected from yeast-displayed libraries that improve trimer-specific antibody recognition.

In summary, the d-SOSIP gp140 variants evolved and the platform and approach described here provide a step forward toward the development of promising novel HIV immunogens, which could be rapidly and iteratively evaluated in immunization studies in animal models. Such evaluation could help elucidate the value of whole envelope strategies relative to subtractive approaches focusing on a restricted set of epitopes. A less hydrophobic fusion peptide proved to be a critical feature to achieve an initial detectable expression level allowing for yeast display-based cell sorting. The shuffling of accumulated mutations and backcrossing to wild type greatly boosted binding to the target HIV mAbs and potentially eliminated deleterious mutations. Variants with further improved binding to certain HIV bnAbs or their germline precursors, following the concept of B-cell-lineage immunogen design [80,81] may be evolved relatively quickly using the approach described here. Glyco-engineered yeast strains [82] could serve as hosts for future yeast-based display systems to select spike protein variants homogeneously decorated with human-like glycan that is involved in binding of many bnAb-classes such as pg9/16[24] or pgt121–123 [56]. Such evolved yeast-produced spike protein derivatives

may also be well suited for solving additional spike protein structures, facilitating rational vaccine design approaches, and further contributing to the immunogen pipeline.

Materials and Methods

General

PCR products were prepared using proofreading Phusion DNA polymerase (Finnzymes) and oligonucleotide primers from Integrated DNA Technologies, unless otherwise stated. DNA restriction and modifying enzymes were from New England Biolabs. PCR products were purified and gel-extracted using kits from either Qiagen or Geneaid. DNA sequences of all constructs were verified using an Applied Biosystems Model 3100 DNA sequencer. *E. coli* strain DH5 alpha was used as host for molecular cloning. Yeast strains *S. cerevisiae* YVH10 or *P. pastoris* SuperMan5 (Research Corporation Technologies) were used as hosts for soluble protein secretion and *S. cerevisiae* EBY100 for cell surface display.

Preparation of DNA constructs

Plasmids pBGP1-JRFL-gp120, pBGP1-JRFL-gp41 and pBGP1-JRFL-gp41dFP for soluble protein secretion in *P. pastoris* strains were prepared as follows. HIV-1 JR-FL gp120, gp41 and gp41dFP were amplified from pPPI4-JRFL-SOSIPopt_R6 gp140[36] using primers JRFL-for2 and JRFLgp120-rev2, JRFLgp41-for2 and JRFL-rev3 or JRFLgp41dFP-for and JRFL-rev3 and inserted between the EcoRI and XbaI sites of pBGP1[83]. Plasmids pRS-JRFL-gp140, pRS-JRFL-gp120H and pRS-JRFL-gp120 for soluble protein secretion in *S. cerevisiae* YVH10 were prepared by amplification of gp140, gp120H or gp120 using primers JRFL-for and JRFL-rev2, JRFL-for and JRFLgp120H-rev or JRFL-for and JRFLgp120-rev and insertion between EagI and BamHI sites of pRS-4G[47]. For plasmid pRS-d-SOSIP, a yeast codon-optimized and designed HIV-1 JRFL gp140, denoted d-SOSIP, based on JRFL-SOSIPopt_R6 gp140[36] was constructed (DNA2.0) and inserted between EagI and BamHI sites of pRS-4G. The DNA sequence of d-SOSIP is shown in S6 Fig. Plasmid pCHA was obtained as a kind gift from Jordi Mata-Fink [47]. Plasmids pCHA-d-SOSIP and pCHA-JRFL-gp120 for *S. cerevisiae* cell surface display were prepared by amplification of gp140 or gp120 from pRS-d-SOSIP using primers gp120co-for and gp140co-rev or gp120co-rev and insertion of PCR products between NheI and BamHI sites of pCHA, resulting in an orientation of HA tag, d-SOSIP, c-myc tag, followed by Aga2p from the N to C termini, respectively. pRS-d-SOSIP-D368R was prepared using primers JRFLD368R-for and JRFLD368R-rev, following the Quikchange site-directed mutagenesis procedure (Agilent). PCR primers are listed in S1 Table.

Protein production and purification

For secretion of soluble HIV spike protein variants lacking any cell-wall anchoring domain from *P. pastoris* SuperMan5, electro-competent yeast cells were prepared as described previously[84], transformed with pBGP1 constructs, plated on YPD plates containing 100 μg/l Zeocin (Invivo Gen) and incubated at 30° C for 3 days to obtain single clones. Typically 2 to 200 ml YPD cultures containing 100 μg/l Zeocin were inoculated to an OD600 of 0.1 from over-night pre-cultures and grown for 6 h at 30° C followed by 5 days at 20° C for constitutive protein expression. For secretion of soluble HIV spike protein variants lacking any cell-wall anchoring domain from *S. cerevisiae* YVH10, chemically competent yeast cells were prepared and transformed with pRS constructs using the Frozen-EZ Yeast Transformation II kit (Zymo), plated onSD-CAA plates supplemented with 40 mg/L L-Tryptophan and incubated at 30° C for 3 days to obtain single clones. Typically, 2 to 50 ml SDCAA cultures supplemented with 40 mg/L

L-Tryptophan were inoculated from over-night pre-cultures to an OD600 of 0.2 and grown for 6 h at 30° C. For induction of protein production, cells were spun down, suspended in 200 ml SGCAA medium containing 40 mg/L L-Tryptophan and grown for 5 days at 20° C. Media compositions have been described previously[84]. Secreted spike protein variants were either detected directly in culture supernatant or IMAC-purified and buffer-exchanged to PBS prior to further analysis.

Yeast cell surface display and flow-cytometric analysis

HIV spike protein variants were displayed on S. cerevisiae EBY100 as decribed previously[47]. Briefly, *S. cerevisiae* was transformed with pCHA constructs using the Frozen-EZ Yeast Transformation II kit (Zymo) and clones were grown on SDCAA plates at 30° C. Typically 2 ml SDCAA medium was inoculated to an OD600 of 0.2 from an over-night pre-culture, grown at 30° C for 6 h, transferred to SGCAA medium and grown for 12 to 18 h at 30° C. Induced cells were analyzed for cell surface display on a MACSQuant Analyzer (Miltenyi Biotec). Typically 10^7 yeast cells were suspended in 200 µl PBS supplemented with 0.1% BSA (PBSF) in 96-well plates (Greiner), spun down for 4 min at 2500 g and supernatant was removed by vacuum aspiration. Cells were the suspended in 50 µl PBSF containing 1:200 dilutions of mouse monoclonal anti-HA tag antibody HA.11 clone 16B12 (Covance) or chicken polyclonal anti-cMyc tag antibody (Gallus Immunotechnology) for detection of display levels, and human HIV antibody at various concentration and incubated for 1 h at ambient temperature while shaking at 1000 rpm. Cells were then washed twice with 200 µl PBSF, suspended in 50 µl PBSF containing 1:200 dilutions of polyclonal goat anti-mouse or goat anti-chicken antibody and goat anti-human antibody conjugated to Alexa488 or Alexa647 (Life Sciences) and incubated for 20 min at ambient temperature while shaking. Cells were again washed once, suspended in 200 µl PBSF, respectively, and kept cold for flow-cytometric analyses. Routinely, cells were gated using forward- and side scatters and median fluorescence intensities (MFIs) were determined from 10,000 scatter-gated events that were then gated for display signal. The gate for display level was set using a non-displaying control sample, assuring that non-displaying cells are excluded. MFI values associated with antibody binding were then normalized to display level by division with the MFI associated with expression tag (nMFIs). All analyses were performed using MACSQuantify software (Miltenyi).

SDS-PAGE and Western blotting analyses

Yeast-secreted and IMAC purified gp120 was denatured for 5 min at 95° C, loaded on a NuPAGE Novex 3–8% Tris-Acetate gel (Life Scienes), and 150 V were applied for 1 h in MOPS buffer (Life Sciences). The gel was stained using GelCode Blue Stain Reagent (Pierce) and analyzed using a Gel Doc XR System (Bio-Rad). For Western blotting analyses of HIV spike protein variants, typically 20 µl of denatured and reduced crude culture supernatant were loaded and the gel was blotted for 1.5 h at 30 V on a 0.45 µm pore-size PVDF membrane (Life Sciences). The membrane was washed twice for 10 min in PBS, blocked for 1 h in PBS supplemented with 5% BSA and 0.1% v/v Tween 20, washed twice for 10 min in PBS supplemented with 0.05% v/v Tween 20 (PBST) and once in PBS. The washed membrane was incubated with 1 ml PBS containing 3% BSA, 0.1% v/v Tween 20 and 5 µl goat polyclonal anti-gp120 antibody HRP conjugate ab53840 (Abcam) for gp120 detection or 1 µl mouse monoclonal anti-His antibody HRP Conjugate 34460 (Qiagen) for His-tag detection while covered by a transparency. The membrane was then washed as before and incubated for 1 min with enhanced chemiluminescence substrate (Pierce) and analyzed using the Gel Doc XR System (Bio-Rad).

HIV-1 gp140 library preparation

JR-FL gp140 library insert was prepared based on a protocol by Fromant *et al.* [85], aiming for 5 amino acid mutations per gene. A 100 μl reaction containing 230 μM dATP, 200 μM dCTP, 420 μM dGTP, 2.9 mM dTTP, 512 pM pCHA-d-SOSIP template DNA, 500 nM primer epyd-for2 and 500 nM primer epyd-rev2, 5 μg/ml BSA, 3.95 mM MgCl2, 500 μM MnCl2, 5 u Taq DNA polymerase (NEB) in 50 mM KCl and 10 mM Tris-HCl pH 8.7 at 25° C. Thermo-cycling conditions were 94° C for 5 min, followed by 16 cycles of 94° C for 1 min, 65° C for 1 min and 72° C for 4 min, and finally 72° C for 10 min. PCR products were column-purified and 200 to 800 ng were used as template for amplification in 1000 to 4000 μl of total PCR reaction volume using Phusion DNA polymerase and primers epyd-for3 and epyd-rev3. Thermocycling conditions were 98° C for 1 min, followed by 35 cycles of 98° C for 10 s, 60° C for 30 s and 72° C for 1 min, and finally 72° C for 10 min. Library vector was prepared by cleaving 250 μg of pCHA-SOSIP-JRFL-gp140-design5 with 400 u of BamHI and NheI, respectively, in 1 ml final volume for 8 h at 37° C, followed by the addition of another 400 u of each enzyme, DTT to 1 mM and incubation over night at 37° C. The reaction was heat-inactivated for 20 min at 65° C. Vector was gel-extracted using a DNA Extraction Maxi Kit (Geneaid). Both insert and vector preparations were ethanol-precipitated, washed and concentrated with Pellet Paint Co-Precipitant (Millipore) and suspended in a final volume of approximately 200 μl (insert) and 80 μl (vector). A total of 1200 μl electrocompetent *S. cerevisiae* EBY100 were prepared essentially as described previously[84], mixed with all insert and vector, split in eight 2 mm cuvettes and transformed at 1.2 kV and 25 uF using a Gene Pulser Xcell (Bio-Rad). Transformed cells were grown in typically 500 ml SDCAA medium and passaged at least once prior to induction and FACS. Library size was determined by plating dilutions of the transformation on SDCAA plates and counting colonies.

DNA shuffling

DNA encoding the enriched and designed gp140 variants was shuffled based on a protocol by Stemmer[86]. Briefly, 2.5 μg of gp140 PCR products were incubated with 1 u DNAseI in 50 μl for exactly 2 min at 24° C, respectively, followed by immediate heat-inactivation at 75° C for 10 min. Reactions were separated on a 2% agarose gel and fragments between 25 bp and 1 kb were gel-extracted. Approximately 80 ng of digested, selected gp140 pool was assembled with 80 ng of digested, initial d-SOSIP in 20 μl reactions using Phusion DNA polymerase and 30 s at 98° C followed by 40 cycles of 10 s at 98° C, 30 s at 55° C, 45 s at 72° C and finally 10 min at 72° C. Exactly 2 μl of assembly products were amplified in 50 μl reactions using primers epyd-for3, epyd-rev3 and phusion DNA polymerase during 1 min at 98° C, 30 cycles of 10 s at 98° C, 30 s at 60° C and 1 min at 72° C and finally 5 min at 72° C. The assembled PCR product was ethanol-precipitated, washed, concentrated and used for library preparation as described in the previous section.

Library selection

Freshly grown yeast libraries were diluted to an OD600 of 0.2 while oversampling the library size at least 10-fold and grown for at least 6 h at 30° C while shaking at 250 rpm. Cells were sedimented, suspended in SGCAA medium and induced for at least 12 h at 30° C. Induced cells were filtered using a 40 μm mesh (BD biosciences) and typically $2x10^8$ cells were washed 3 times with 1 ml PBSF and incubated for 1 h at ambient temperature with varying concentrations of HIV antibodies (Table 1) and optionally a 1:200 dilution of chicken polyclonal anti-cMyc tag antibody (Gallus Immunotechnology) in 500 μl PBSF. Cells were washed twice with 1 ml PBSF and stained for 20 min on ice with 1:200 dilutions of goat anti-human polyclonal

antibody conjugated to Alexa647 (Life Sciences) and optionally goat anti-chicken polyclonal antibody conjugated to Alexa488 (Life Sciences), while shielded from light. Cells were washed twice, split in four aliquots and kept as pellets on ice and shielded from light until sorting. FACS was performed using an iCyt sy3200 cell sorter system (Sony). Briefly, aliquots of typically $4x10^7$ stained yeast cells were suspended in 2 ml PBSF and sorted at around 10,000 events/s using 0.1% to 5% sorting gates in recovery mode during initial and ultra purity mode during later sort cycles. Typical sorting gates for initial and later selection rounds are shown in S2 Fig.. Sorted cells were suspended in SDCAA medium and grown for 12 to 36 h for subsequent sorting rounds or analyses of selected pools.

Biosensor binding studies

All binding analyses were performed at 25° C using an Octet RED96 System (ForteBio), 1000 rpm shaking speed and PBS containing 0.1% BSA, 0.02% v/v Tween20 as sample buffer. Protein A-coated biosensor tips were loaded for 10 min with 10 µg/ml IgG, dipped in buffer and probed with 500 nM gp120 for 8 min, followed by a dissociation phase of 5 min in buffer. A trace obtained from IgG probed with buffer only was subtracted as reference.

Molecular Modelling

The gp120 crystal structure used for modeling was taken from 4NCO chain A. The CD4-binding site was determined using PyMol interface residues script on gp120-CD4 co-crystal structure PDB ID: 1GC1 and mapped to the corresponding side chains on 4NCO. Mutations of d-SOSIP picked up during selections were mapped onto the BG505 gp140.664 SOSIP structure *via* sequence alignment. Side chain rotamers with minimal clashes were chosen. Hydrogen bonds were designated at distance of <4 Å and >2 Å. Mutation D180N and those in gp41 were not mapped due to lack of resolution in the crystal structure.

Supporting Information

S1 Fig. Characterization of yeast-secreted gp120. (A) SDS-PAGE analysis of JR-FL gp120 secreted from either *S. cerevisiae* strain YVH10 (1) or *P. pastoris* strain SuperMan5 (2). (B) Octet biosensor binding analysis of *S. cerevisiae* or *P. pastoris*-secreted gp120. Maximum binding responses during association phase are plotted in nm for a panel of HIV gp120 antibodies and human IgG1 (hIgG1) as reference. (C) Western blotting detection of *S. cerevisiae*-secreted and SOSIP gp140 or d-SOSIP with and without PNGase F-treatment to remove N-linked glycans, the black vertical line separates non-adjacent lanes originating from the same blot.
(TIFF)

S2 Fig. FACS gate settings. Representative sort gates used during FACS. 100,000 events were recorded, respectively and selection rounds are annotated. Percentages of gated cells are indicated within the respective gates.
(TIFF)

S3 Fig. Sequence clustering analysis. Clones sequenced after selection cycle 3.3 and before DNA shuffling (A) or directly after DNA shuffling (B) were clustered using a Blossum90 matrix. Lengths of the branches correlate with sequence similarity. Sequence clusters observed after C3.3 are denoted.
(TIFF)

S4 Fig. Pool binding analysis of different selection tracks. Expression-normalized binding response for selection cycle 3.3 track 1 (grey), 4.3 tracks 1 (black), 2 (green) and 3 (blue) are

plotted against logarithmic Ab concentrations for VRC01 and PGV04.
(TIFF)

S5 Fig. Sequence alignment of lead candidates. Amino acid sequence of d-SOSIP. Residues mutated in clones 3.3.1, 4.3.B01 (B01) and 4.3.D01 (D01) are annotated. The designed Kex2 site is underlined and the designed fusion peptide written in bold letters. The lysine to glutamine mutation to remove an internal, predicted Kex2 site is underlined and bolded.
(TIFF)

S6 Fig. d-SOSIP nucleotide sequence. The nucleotide sequence of d-SOSIP gp140 compatible with the primers used in this study is shown.
(TIFF)

S7 Fig. Binding analysis of yeast-secreted, soluble gp120 and gp140. Yeast-secreted and purified JR-FL g120 (black) and 4.3.D01 gp140 (grey) were probed for binding to HIV mAb NIH45–46 G54W. The BioLayer Interferometry (BLI) binding response is plotted in nm.
(TIFF)

S1 Table. Primers utilized in gene and library construction.
(DOCX)

S2 Table. Raw data summary of Fig. 2D.
(DOCX)

Acknowledgments

Author Contributions

Conceived and designed the experiments: SKG MBB MEA. Performed the experiments: SKG MBB. Analyzed the data: SKG MBB MEA. Wrote the paper: SKG MBB MEA.

References

1. Hoxie JA (2010) Toward an antibody-based HIV-1 vaccine. Annu Rev Med 61: 135–152. doi: 10.1146/annurev.med.60.042507.164323 PMID: 19824826

2. Walker LM, Burton DR (2010) Rational antibody-based HIV-1 vaccine design: current approaches and future directions. Curr Opin Immunol 22: 358–366. doi: 10.1016/j.coi.2010.02.012 PMID: 20299194

3. McElrath MJ, Haynes BF (2010) Induction of immunity to human immunodeficiency virus type-1 by vaccination. Immunity 33: 542–554. doi: 10.1016/j.immuni.2010.09.011 PMID: 21029964

4. Binley JM, Ban YE, Crooks ET, Eggink D, Osawa K, et al. (2010) Role of complex carbohydrates in human immunodeficiency virus type 1 infection and resistance to antibody neutralization. J Virol 84: 5637–5655. doi: 10.1128/JVI.00105-10 PMID: 20335257

5. Frey G, Peng H, Rits-Volloch S, Morelli M, Cheng Y, et al. (2008) A fusion-intermediate state of HIV-1 gp41 targeted by broadly neutralizing antibodies. Proc Natl Acad Sci U S A 105: 3739–3744. doi: 10.1073/pnas.0800255105 PMID: 18322015

6. Haynes BF, Fleming J, St Clair EW, Katinger H, Stiegler G, et al. (2005) Cardiolipin polyspecific auto-reactivity in two broadly neutralizing HIV-1 antibodies. Science 308: 1906–1908. PMID: 15860590

7. Labrijn AF, Poignard P, Raja A, Zwick MB, Delgado K, et al. (2003) Access of antibody molecules to the conserved coreceptor binding site on glycoprotein gp120 is sterically restricted on primary human immunodeficiency virus type 1. J Virol 77: 10557–10565. PMID: 12970440

8. Mouquet H, Scheid JF, Zoller MJ, Krogsgaard M, Ott RG, et al. (2010) Polyreactivity increases the apparent affinity of anti-HIV antibodies by heteroligation. Nature 467: 591–595. doi: 10.1038/nature09385 PMID: 20882016

9. Richman DD, Wrin T, Little SJ, Petropoulos CJ (2003) Rapid evolution of the neutralizing antibody response to HIV type 1 infection. Proc Natl Acad Sci U S A 100: 4144–4149. PMID: 12644702

10. Schief WR, Ban YE, Stamatatos L (2009) Challenges for structure-based HIV vaccine design. Curr Opin HIV AIDS 4: 431–440. doi: 10.1097/COH.0b013e32832e6184 PMID: 20048708

11. Wei X, Decker JM, Wang S, Hui H, Kappes JC, et al. (2003) Antibody neutralization and escape by HIV-1. Nature 422: 307–312. PMID: 12646921

12. Klausner RD, Fauci AS, Corey L, Nabel GJ, Gayle H, et al. (2003) Medicine. The need for a global HIV vaccine enterprise. Science 300: 2036–2039. PMID: 12829768

13. Van Regenmortel MH (2011) Limitations to the structure-based design of HIV-1 vaccine immunogens. J Mol Recognit 24: 741–753. doi: 10.1002/jmr.1116 PMID: 21812050

14. Liao HX, Lynch R, Zhou T, Gao F, Alam SM, et al. (2013) Co-evolution of a broadly neutralizing HIV-1 antibody and founder virus. Nature 496: 469–476. doi: 10.1038/nature12053 PMID: 23552890

15. Ackerman M, Alter G (2013) Mapping the journey to an HIV vaccine. The New England journal of medicine 369: 389–391. doi: 10.1056/NEJMcibr1304437 PMID: 23883384

16. Doria-Rose NA, Schramm CA, Gorman J, Moore PL, Bhiman JN, et al. (2014) Developmental pathway for potent V1V2-directed HIV-neutralizing antibodies. Nature 509: 55–62. doi: 10.1038/nature13036 PMID: 24590074

17. Moore PL, Gray ES, Wibmer CK, Bhiman JN, Nonyane M, et al. (2012) Evolution of an HIV glycan-dependent broadly neutralizing antibody epitope through immune escape. Nature medicine 18: 1688–1692. doi: 10.1038/nm.2985 PMID: 23086475

18. Binley JM, Wrin T, Korber B, Zwick MB, Wang M, et al. (2004) Comprehensive cross-clade neutralization analysis of a panel of anti-human immunodeficiency virus type 1 monoclonal antibodies. J Virol 78: 13232–13252. PMID: 15542675

19. Burton DR, Pyati J, Koduri R, Sharp SJ, Thornton GB, et al. (1994) Efficient neutralization of primary isolates of HIV-1 by a recombinant human monoclonal antibody. Science 266: 1024–1027. PMID: 7973652

20. Mikell I, Sather DN, Kalams SA, Altfeld M, Alter G, et al. (2011) Characteristics of the earliest cross-neutralizing antibody response to HIV-1. PLoS Pathog 7: e1001251. doi: 10.1371/journal.ppat.1001251 PMID: 21249232

21. Stiegler G, Kunert R, Purtscher M, Wolbank S, Voglauer R, et al. (2001) A potent cross-clade neutralizing human monoclonal antibody against a novel epitope on gp41 of human immunodeficiency virus type 1. AIDS Res Hum Retroviruses 17: 1757–1765. PMID: 11788027

22. Trkola A, Purtscher M, Muster T, Ballaun C, Buchacher A, et al. (1996) Human monoclonal antibody 2G12 defines a distinctive neutralization epitope on the gp120 glycoprotein of human immunodeficiency virus type 1. J Virol 70: 1100–1108. PMID: 8551569

23. Corti D, Langedijk JP, Hinz A, Seaman MS, Vanzetta F, et al. (2010) Analysis of memory B cell responses and isolation of novel monoclonal antibodies with neutralizing breadth from HIV-1-infected individuals. PLoS One 5: e8805. doi: 10.1371/journal.pone.0008805 PMID: 20098712

24. Walker LM, Phogat SK, Chan-Hui PY, Wagner D, Phung P, et al. (2009) Broad and potent neutralizing antibodies from an African donor reveal a new HIV-1 vaccine target. Science 326: 285–289. doi: 10.1126/science.1178746 PMID: 19729618

25. Wu X, Yang ZY, Li Y, Hogerkorp CM, Schief WR, et al. (2010) Rational design of envelope identifies broadly neutralizing human monoclonal antibodies to HIV-1. Science 329: 856–861. doi: 10.1126/science.1187659 PMID: 20616233

26. Blattner C, Lee JH, Sliepen K, Derking R, Falkowska E, et al. (2014) Structural Delineation of a Quaternary, Cleavage-Dependent Epitope at the gp41-gp120 Interface on Intact HIV-1 Env Trimers. Immunity.

27. Falkowska E, Le KM, Ramos A, Doores KJ, Lee JH, et al. (2014) Broadly Neutralizing HIV Antibodies Define a Glycan-Dependent Epitope on the Prefusion Conformation of gp41 on Cleaved Envelope Trimers. Immunity.

28. Antipov E, Cho AE, Wittrup KD, Klibanov AM (2008) Highly L and D enantioselective variants of horseradish peroxidase discovered by an ultrahigh-throughput selection method. Proc Natl Acad Sci U S A 105: 17694–17699. doi: 10.1073/pnas.0809851105 PMID: 19004779

29. Hackel BJ, Kapila A, Wittrup KD (2008) Picomolar affinity fibronectin domains engineered utilizing loop length diversity, recursive mutagenesis, and loop shuffling. J Mol Biol 381: 1238–1252. doi: 10.1016/j.jmb.2008.06.051 PMID: 18602401

30. Boder ET, Wittrup KD (2000) Yeast surface display for directed evolution of protein expression, affinity, and stability. Methods Enzymol 328: 430–444. PMID: 11075358

31. Shusta EV, Kieke MC, Parke E, Kranz DM, Wittrup KD (1999) Yeast polypeptide fusion surface display levels predict thermal stability and soluble secretion efficiency. J Mol Biol 292: 949–956. PMID: 10512694

32. Boder ET, Midelfort KS, Wittrup KD (2000) Directed evolution of antibody fragments with monovalent femtomolar antigen-binding affinity. Proc Natl Acad Sci U S A 97: 10701–10705. PMID: 10984501

33. McGuire AT, Hoot S, Dreyer AM, Lippy A, Stuart A, et al. (2013) Engineering HIV envelope protein to activate germline B cell receptors of broadly neutralizing anti-CD4 binding site antibodies. The Journal of experimental medicine 210: 655–663. doi: 10.1084/jem.20122824 PMID: 23530120

34. Jardine J, Julien JP, Menis S, Ota T, Kalyuzhniy O, et al. (2013) Rational HIV immunogen design to target specific germline B cell receptors. Science 340: 711–716. doi: 10.1126/science.1234150 PMID: 23539181

35. Schulke N, Vesanen MS, Sanders RW, Zhu P, Lu M, et al. (2002) Oligomeric and conformational properties of a proteolytically mature, disulfide-stabilized human immunodeficiency virus type 1 gp140 envelope glycoprotein. Journal of virology 76: 7760–7776. PMID: 12097589

36. Sanders RW, Vesanen M, Schuelke N, Master A, Schiffner L, et al. (2002) Stabilization of the soluble, cleaved, trimeric form of the envelope glycoprotein complex of human immunodeficiency virus type 1. Journal of virology 76: 8875–8889. PMID: 12163607

37. Binley JM, Sanders RW, Clas B, Schuelke N, Master A, et al. (2000) A recombinant human immunodeficiency virus type 1 envelope glycoprotein complex stabilized by an intermolecular disulfide bond between the gp120 and gp41 subunits is an antigenic mimic of the trimeric virion-associated structure. Journal of virology 74: 627–643. PMID: 10623724

38. Lyumkis D, Julien JP, de Val N, Cupo A, Potter CS, et al. (2013) Cryo-EM structure of a fully glycosylated soluble cleaved HIV-1 envelope trimer. Science 342: 1484–1490. doi: 10.1126/science.1245627 PMID: 24179160

39. Julien JP, Cupo A, Sok D, Stanfield RL, Lyumkis D, et al. (2013) Crystal structure of a soluble cleaved HIV-1 envelope trimer. Science 342: 1477–1483. doi: 10.1126/science.1245625 PMID: 24179159

40. Ringe RP, Sanders RW, Yasmeen A, Kim HJ, Lee JH, et al. (2013) Cleavage strongly influences whether soluble HIV-1 envelope glycoprotein trimers adopt a native-like conformation. Proceedings of the National Academy of Sciences of the United States of America 110: 18256–18261. doi: 10.1073/pnas.1314351110 PMID: 24145402

41. Sanders RW, Derking R, Cupo A, Julien JP, Yasmeen A, et al. (2013) A next-generation cleaved, soluble HIV-1 Env Trimer, BG505 SOSIP.664 gp140, expresses multiple epitopes for broadly neutralizing but not non-neutralizing antibodies. PLoS pathogens 9: e1003618. doi: 10.1371/journal.ppat.1003618 PMID: 24068931

42. Boder ET, Wittrup KD (1997) Yeast surface display for screening combinatorial polypeptide libraries. Nature biotechnology 15: 553–557. PMID: 9181578

43. Rakestraw JA, Aird D, Aha PM, Baynes BM, Lipovsek D (2011) Secretion-and-capture cell-surface display for selection of target-binding proteins. Protein engineering, design & selection: PEDS 24: 525–530. doi: 10.1016/j.vaccine.2015.01.040 PMID: 25629524

44. Boder ET, Bill JR, Nields AW, Marrack PC, Kappler JW (2005) Yeast surface display of a noncovalent MHC class II heterodimer complexed with antigenic peptide. Biotechnology and bioengineering 92: 485–491. PMID: 16155952

45. Kim YS, Bhandari R, Cochran JR, Kuriyan J, Wittrup KD (2006) Directed evolution of the epidermal growth factor receptor extracellular domain for expression in yeast. Proteins 62: 1026–1035. PMID: 16355407

46. Han T, Sui J, Bennett AS, Liddington RC, Donis RO, et al. (2011) Fine epitope mapping of monoclonal antibodies against hemagglutinin of a highly pathogenic H5N1 influenza virus using yeast surface

display. Biochemical and biophysical research communications 409: 253–259. doi: 10.1016/j.bbrc. 2011.04.139 PMID: 21569761

47. Mata-Fink J, Kriegsman B, Yu HX, Zhu H, Hanson MC, et al. (2013) Rapid conformational epitope mapping of anti-gp120 antibodies with a designed mutant panel displayed on yeast. Journal of molecular biology 425: 444–456. doi: 10.1016/j.jmb.2012.11.010 PMID: 23159556

48. Brien JD, Austin SK, Sukupolvi-Petty S, O'Brien KM, Johnson S, et al. (2010) Genotype-specific neutralization and protection by antibodies against dengue virus type 3. Journal of virology 84: 10630–10643. doi: 10.1128/JVI.01190-10 PMID: 20702644

49. Zhang X, Wang J, Wen K, Mou Z, Zou L, et al. (2009) Antibody binding site mapping of SARS-CoV spike protein receptor-binding domain by a combination of yeast surface display and phage peptide library screening. Viral immunology 22: 407–415. doi: 10.1089/vim.2009.0046 PMID: 19951177

50. Oliphant T, Nybakken GE, Engle M, Xu Q, Nelson CA, et al. (2006) Antibody recognition and neutralization determinants on domains I and II of West Nile Virus envelope protein. Journal of virology 80: 12149–12159. PMID: 17035317

51. Sabo MC, Luca VC, Prentoe J, Hopcraft SE, Blight KJ, et al. (2011) Neutralizing monoclonal antibodies against hepatitis C virus E2 protein bind discontinuous epitopes and inhibit infection at a postattachment step. Journal of virology 85: 7005–7019. doi: 10.1128/JVI.00586-11 PMID: 21543495

52. De Pourcq K, De Schutter K, Callewaert N (2010) Engineering of glycosylation in yeast and other fungi: current state and perspectives. Applied microbiology and biotechnology 87: 1617–1631. doi: 10.1007/s00253-010-2721-1 PMID: 20585772

53. Jacobs PP, Geysens S, Vervecken W, Contreras R, Callewaert N (2009) Engineering complex-type N-glycosylation in Pichia pastoris using GlycoSwitch technology. Nature protocols 4: 58–70. doi: 10.1038/nprot.2008.213 PMID: 19131957

54. Hamilton SR, Bobrowicz P, Bobrowicz B, Davidson RC, Li H, et al. (2003) Production of complex human glycoproteins in yeast. Science 301: 1244–1246. PMID: 12947202

55. Villalobos A, Ness JE, Gustafsson C, Minshull J, Govindarajan S (2006) Gene Designer: a synthetic biology tool for constructing artificial DNA segments. BMC bioinformatics 7: 285. PMID: 16756672

56. Walker LM, Huber M, Doores KJ, Falkowska E, Pejchal R, et al. (2011) Broad neutralization coverage of HIV by multiple highly potent antibodies. Nature 477: 466–470. doi: 10.1038/nature10373 PMID: 21849977

57. Scheid JF, Mouquet H, Ueberheide B, Diskin R, Klein F, et al. (2011) Sequence and structural convergence of broad and potent HIV antibodies that mimic CD4 binding. Science 333: 1633–1637. doi: 10.1126/science.1207227 PMID: 21764753

58. Pantophlet R, Ollmann Saphire E, Poignard P, Parren PW, Wilson IA, et al. (2003) Fine mapping of the interaction of neutralizing and nonneutralizing monoclonal antibodies with the CD4 binding site of human immunodeficiency virus type 1 gp120. Journal of virology 77: 642–658. PMID: 12477867

59. Wu X, Zhou T, Zhu J, Zhang B, Georgiev I, et al. (2011) Focused evolution of HIV-1 neutralizing antibodies revealed by structures and deep sequencing. Science 333: 1593–1602. doi: 10.1126/science.1207532 PMID: 21835983

60. Crameri A, Raillard SA, Bermudez E, Stemmer WP (1998) DNA shuffling of a family of genes from diverse species accelerates directed evolution. Nature 391: 288–291. PMID: 9440693

61. Plotkin SA (2010) Correlates of protection induced by vaccination. Clinical and vaccine immunology: CVI 17: 1055–1065. doi: 10.1128/CVI.00131-10 PMID: 20463105

62. Wyatt R, Sodroski J (1998) The HIV-1 envelope glycoproteins: fusogens, antigens, and immunogens. Science 280: 1884–1888. PMID: 9632381

63. Chen L, Kwon YD, Zhou T, Wu X, O'Dell S, et al. (2009) Structural basis of immune evasion at the site of CD4 attachment on HIV-1 gp120. Science 326: 1123–1127. doi: 10.1126/science.1175868 PMID: 19965434

64. Klein JS, Bjorkman PJ (2010) Few and far between: how HIV may be evading antibody avidity. PLoS pathogens 6: e1000908. doi: 10.1371/journal.ppat.1000908 PMID: 20523901

65. Saphire EO, Montero M, Menendez A, van Houten NE, Irving MB, et al. (2007) Structure of a high-affinity "mimotope" peptide bound to HIV-1-neutralizing antibody b12 explains its inability to elicit gp120 cross-reactive antibodies. Journal of molecular biology 369: 696–709. PMID: 17445828

66. Pantophlet R, Wilson IA, Burton DR (2004) Improved design of an antigen with enhanced specificity for the broadly HIV-neutralizing antibody b12. Protein engineering, design & selection: PEDS 17: 749–758. doi: 10.1016/j.vaccine.2015.01.040 PMID: 25629524

67. Dai K, Boyington JC, Shi W, Schmidt SD, Georgiev I, et al. (2012) Hyperglycosylated resurfaced stabilized GP120 core as an immunogen elicits antibodies targeted at the CD4-binding site. Retrovirology 9. doi: 10.1186/1742-4690-9-115 PMID: 23256570

68. Correia BE, Ban YE, Holmes MA, Xu H, Ellingson K, et al. (2010) Computational design of epitope-scaffolds allows induction of antibodies specific for a poorly immunogenic HIV vaccine epitope. Structure 18: 1116–1126. doi: 10.1016/j.str.2010.06.010 PMID: 20826338

69. Ofek G, Guenaga FJ, Schief WR, Skinner J, Baker D, et al. (2010) Elicitation of structure-specific antibodies by epitope scaffolds. Proceedings of the National Academy of Sciences of the United States of America 107: 17880–17887. doi: 10.1073/pnas.1004728107 PMID: 20876137

70. Azoitei ML, Correia BE, Ban YE, Carrico C, Kalyuzhniy O, et al. (2011) Computation-guided backbone grafting of a discontinuous motif onto a protein scaffold. Science 334: 373–376. doi: 10.1126/science.1209368 PMID: 22021856

71. Ahmed FK, Clark BE, Burton DR, Pantophlet R (2012) An engineered mutant of HIV-1 gp120 formulated with adjuvant Quil A promotes elicitation of antibody responses overlapping the CD4-binding site. Vaccine 30: 922–930. doi: 10.1016/j.vaccine.2011.11.089 PMID: 22142583

72. Ackerman ME, Dugast AS, Alter G (2012) Emerging concepts on the role of innate immunity in the prevention and control of HIV infection. Annual review of medicine 63: 113–130. doi: 10.1146/annurev-med-050310-085221 PMID: 22077718

73. Kovacs JM, Nkolola JP, Peng H, Cheung A, Perry J, et al. (2012) HIV-1 envelope trimer elicits more potent neutralizing antibody responses than monomeric gp120. Proceedings of the National Academy of Sciences of the United States of America 109: 12111–12116. doi: 10.1073/pnas.1204533109 PMID: 22773820

74. Morner A, Douagi I, Forsell MN, Sundling C, Dosenovic P, et al. (2009) Human immunodeficiency virus type 1 env trimer immunization of macaques and impact of priming with viral vector or stabilized core protein. Journal of virology 83: 540–551. doi: 10.1128/JVI.01102-08 PMID: 19004960

75. Srivastava IK, Kan E, Sun Y, Sharma VA, Cisto J, et al. (2008) Comparative evaluation of trimeric envelope glycoproteins derived from subtype C and B HIV-1 R5 isolates. Virology 372: 273–290. PMID: 18061231

76. Leaman DP, Zwick MB (2013) Increased functional stability and homogeneity of viral envelope spikes through directed evolution. PLoS pathogens 9: e1003184. doi: 10.1371/journal.ppat.1003184 PMID: 23468626

77. Shusta EV, Kieke MC, Parke E, Kranz DM, Wittrup KD (1999) Yeast polypeptide fusion surface display levels predict thermal stability and soluble secretion efficiency. Journal of molecular biology 292: 949–956. PMID: 10512694

78. Brodsky JL, Skach WR (2011) Protein folding and quality control in the endoplasmic reticulum: Recent lessons from yeast and mammalian cell systems. Current opinion in cell biology 23: 464–475. doi: 10.1016/j.ceb.2011.05.004 PMID: 21664808

79. Rakestraw JA, Baskaran AR, Wittrup KD (2006) A flow cytometric assay for screening improved heterologous protein secretion in yeast. Biotechnology progress 22: 1200–1208. PMID: 16889399

80. Haynes BF, Kelsoe G, Harrison SC, Kepler TB (2012) B-cell-lineage immunogen design in vaccine development with HIV-1 as a case study. Nature biotechnology 30: 423–433. doi: 10.1038/nbt.2197 PMID: 22565972

81. Grimm SK, Ackerman ME (2013) Vaccine design: emerging concepts and renewed optimism. Current opinion in biotechnology 24: 1078–1088. doi: 10.1016/j.copbio.2013.02.015 PMID: 23474232

82. Hamilton SR, Davidson RC, Sethuraman N, Nett JH, Jiang Y, et al. (2006) Humanization of yeast to produce complex terminally sialylated glycoproteins. Science 313: 1441–1443. PMID: 16960007

83. Lee CC, Williams TG, Wong DW, Robertson GH (2005) An episomal expression vector for screening mutant gene libraries in Pichia pastoris. Plasmid 54: 80–85. PMID: 15907541

84. Chao G, Lau WL, Hackel BJ, Sazinsky SL, Lippow SM, et al. (2006) Isolating and engineering human antibodies using yeast surface display. Nature protocols 1: 755–768. PMID: 17406305

85. Fromant M, Blanquet S, Plateau P (1995) Direct random mutagenesis of gene-sized DNA fragments using polymerase chain reaction. Analytical biochemistry 224: 347–353. PMID: 7710092

86. Stemmer WP (1994) DNA shuffling by random fragmentation and reassembly: in vitro recombination for molecular evolution. Proceedings of the National Academy of Sciences of the United States of America 91: 10747–10751. PMID: 7938023